Numerical Analysis on Combustion Instabilities in a Multi-Injector GOX-GCH4 Combustion Chamber

By B. Zhang, B. Wang*† AND XY. Hu‡ AND O. Haidn¶
School of Aerospace Engineering, Tsinghua University, Beijing, China

LOX/LH2 has been widely used in liquid rocket engine for transfer into orbit or space exploration due to its high specific impulse. The potential of using hydrocarbon as propellant, in particular methane instead of hydrogen, is one of the most promising solution for the high operational costs. Developing new fuel type rocket engine also brings new challenges to combustion instabilities. To study combustion instabilities in rocket engine using hydrocarbon as fuel, a compressible LES turbulent combustion parallel solver is used to get numerical simulation results. Test cases are based on experimental data of BKS on the LTF high pressure test stand at TUM, which is a multi-element rocket combustion chamber. Both stable and unstable combustion are observed in the experiment and pressure signals at positions along whole chamber are acquired. For unstable case both experiment and simulation show a dominant frequency about 1400Hz, which is the 1st order longitudinal mode of the combustor. For stable case there are also several frequencies but the amplitude is quite small. Several parameters are studied and we find that for unstable case CH2O(which is mainly involved with ignition process) has the same phase with pressure, OH(which is mainly involved with heat release) has a little phase lag with pressure but less than 90° , meaning that they are still mostly coupled. While for stable case both CH2O and OH has totally different phase with pressure. Also we find that pressure wave will increase the baroclinic term in vorticity equation, thus increasing fuel oxygen mixing and then promote combustion and heat release.

---

1. Introduction

Oxygen/methane is one of the most promising hydrocarbon combination for space propulsion due to its high specific impulse, low coking tendency and high economy efficiency. Design liquid rocket engine using methane as fuel requires detailed knowledge and full understanding about evaporation, atomization, combustion and heat transfer characteristic of hydrocarbon propellant [1].

NASA [2, 3], Russia [4] and Europe [5] have developed LOX/LCH4 engine for booster applications. SpaceX is developing its liquid rocket engine using methane as the fuel for travelling to Mars because there are 5 million cubic km ice and 25 trillion metric tons CO2 on Mars and we can achieve methane regeneration [6]. Developing new fuel type engine also brings new challenges to combustion instabilities, especially in high pressure conditions, which is much worth being studied.

† School of Aerospace Engineering, Tsinghua University
‡ Lehrstuhl für Aerodynamik und Strömungsmechanik, Technische Universität München
¶ Lehrstuhl für Turbomaschinen und Flugantriebe, Technische Universität München

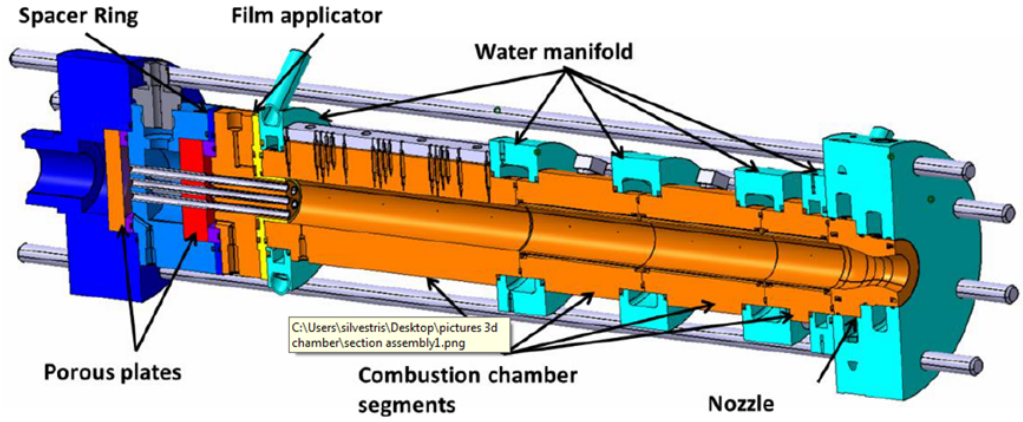

FIGURE 1. Combustion chamber schematic

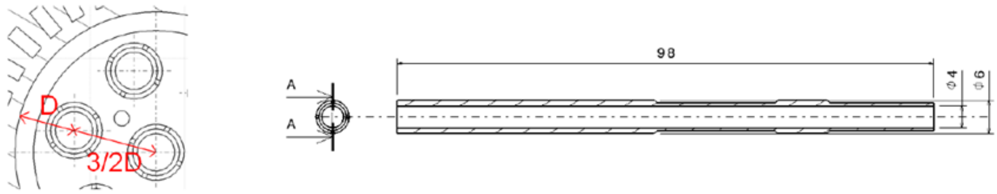

FIGURE 2. Scheme of the injector

To study combustion characteristics of rocket engine using methane as the fuel, O.Haidn et al have done experimental research about single or multi injector GOX/GCH4 combustion chamber [1, 7, 8]. L.Selle et al have done numerical simulation about single injector GOX/GCH4 combustion chamber [9–15]. While hydrocarbon engines are attractive for its low cost, combustion instabilities are still inevitable. Both stable and unstable combustion are observed in a multi-injector GOX/GCH4 combustion chamber called BKS in the LTF high pressure test stand at TUM, in which only OF ratio is different.

Through numerical method we can get more detailed information about flame structure and study mechanism of this unstable combustion. Test cases are based on BKS multi-injector GOX/GCH4 combustion chamber. Geometry of BKS combustion chamber and injector are shown in figure 1 and figure 2. Injector parameters are shown in table 1. Operation conditions are shown in table 2. The operating pressure is 20 bar.Pressure signals at positions along whole chamber are acquired. Figure 3 and figure 4 show dynamic pressure at position located in combustion chamber. We can see combustion in the first case is unstable and the second case is stable.

Figure 5 and figure 6 show the spectrum of dynamic pressure in two cases. In unstable case, the main pressure oscillation frequency is 1410 Hz, 2840 Hz and 4240 Hz, which is exactly the 1st-3rd order longitudinal mode of this combustion chamber (theoretical value: 1409Hz, 2818Hz and 4227Hz). The effects of the 1st order radial mode (theoretical value: 40655 Hz) and the 1st order azimuthal mode (theoretical value: 19535 Hz) can be neglected because they are much higher and much more difficult to excite.

We try to use numerical simulation method to study flame structure and predict combustion instabilities in these cases. For unstable case large amplitude dynamic pressure is also observed in our simulation and the dominant frequency is quite close to exper-

GOX diameter	[mm]	4
GOX post wall thickness	[mm]	0.5
GOX post recess	[mm]	0
GCH4 diameter	[mm]	6
GOX injector length	[mm]	98
GCH4 injector length	[mm]	46
Injector area ratio	[-]	0.76875

TABLE 1. Injector parameters

Test name	Pressure [bar]	T-inlet [K]	OF	Φ	Mdot-OX [kg/s]	Mdot-CH4 [kg/s]	Mdot-tot [kg/s]	Combustion
case1	20	300	2.44	1.640	0.195	0.080	0.275	Unstable
case2	20	300	3.07	1.303	0.228	0.0744	0.3024	Stable

TABLE 2. Operating conditions

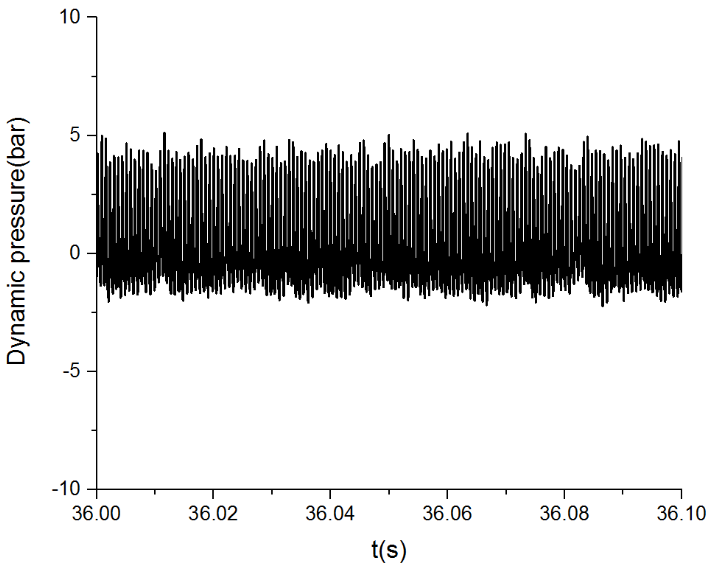

FIGURE 3. Dynamic pressure signal of case1

iment, while for stable case the dynamic pressure is much smaller. We also studied several parameters in this process, trying to reveal the inner mechanism of this combustion instability.

2. Numerical method

Since combustion instabilities in this case mainly show the longitudinal mode rather than the radial or azimuthal mode and 3D unsteady simulation costs too much com-

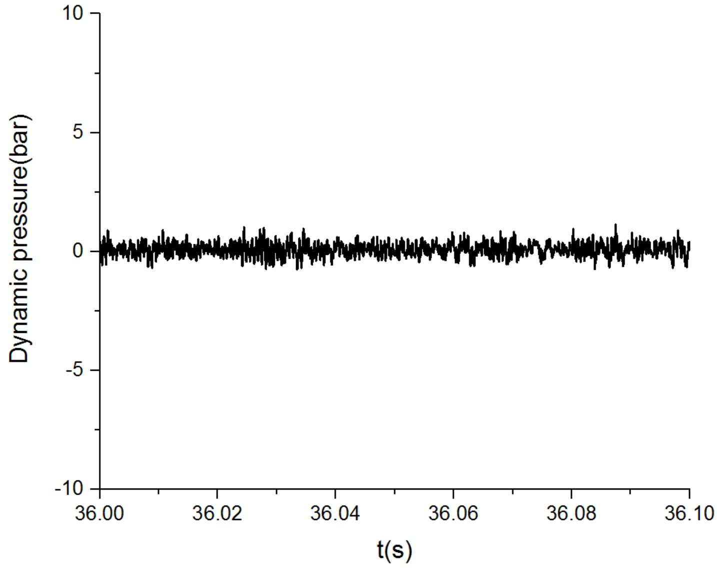

FIGURE 4. Dynamic pressure signal of case2

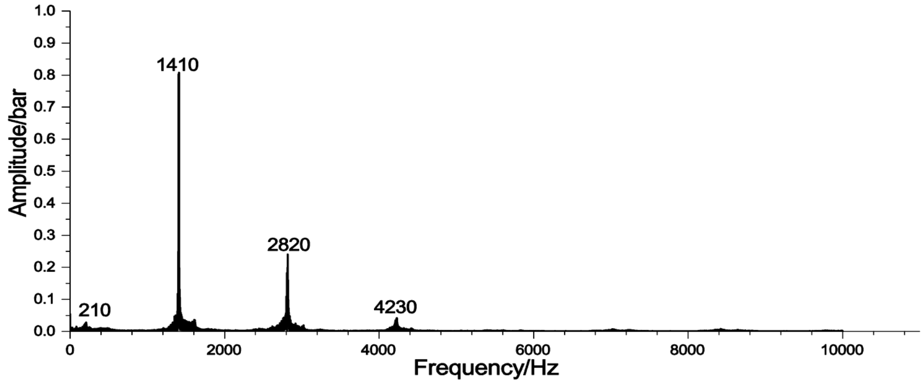

FIGURE 5. Spectrum of dynamic pressure in case1

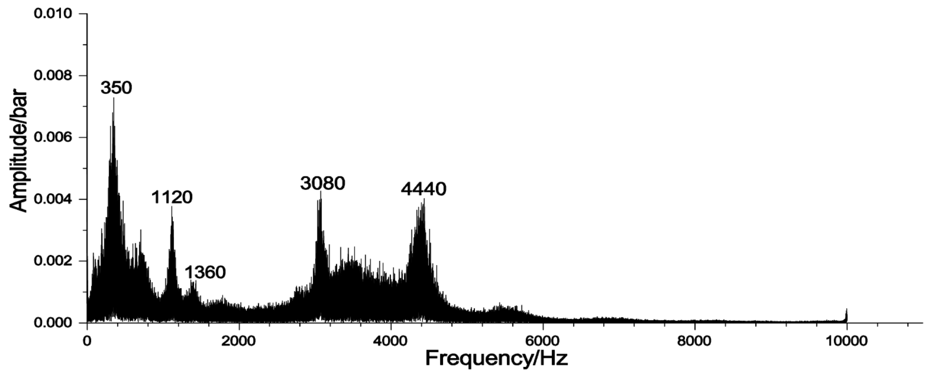

FIGURE 6. Spectrum of dynamic pressure in case2

putation resource, we use 2D simulation to study the flame structure and combustion instabilities.

To simulate the whole process inside the BKS combustion chamber we use RoSim solver developed by Spray Combustion and Propulsion Lab in Tsinghua University. RoSim is a compressible LES turbulent combustion parallel solver.

The formulation is based on the Favre-fltered conservation equations of mass, momentum, and energy in three dimensions. These equations are obtained by fltering the small-scale dynamics from the resolved scales over a well-defined set of spatial and temporal intervals. They can be conveniently expressed in the following Cartesian tensor form:

$$
\begin{aligned}
&\frac{\partial\bar{\rho}}{\partial t}+\frac{\partial\bar{\rho}\tilde{u}_j}{\partial x_i}=0\\
&\frac{\partial\bar{\rho}\tilde{u}_i}{\partial t}+\frac{\partial(\bar{\rho}\tilde{u}_i\tilde{u}_j+\bar{p}\delta_{ij})}{\partial x_j}=\frac{\partial(\tilde{\tau}_{ij}-\tau_{ij}^{sgs})}{\partial x_j}\\
&\frac{\partial\bar{\rho}\tilde{E}}{\partial t}+\frac{\partial[(\bar{\rho}\tilde{E}+\bar{p})\tilde{u}_i)}{\partial x_i}=\frac{\partial}{\partial x_i}(\tilde{u}_j\tilde{\tau}_{ij}+\lambda\frac{\partial\tilde{T}}{\partial x_i}-H_i^{sgs}+\sigma_i^{sgs})\\
&\frac{\partial\bar{\rho}\tilde{E}}{\partial t}+\frac{\partial[(\bar{\rho}\tilde{E}+\bar{p})\tilde{u}_i]}{\partial x_i}=\frac{\partial}{\partial x_i}(\tilde{u}_j\tilde{\tau}_{ij}+\lambda\frac{\partial\tilde{T}}{\partial x_i}-H_i^{sgs}+\sigma_i^{sgs})\\
&\frac{\partial\bar{\rho}\tilde{Y}_k}{\partial t}+\frac{\partial\bar{\rho}\tilde{u}_j\tilde{Y}_k}{\partial x_j}=\frac{\partial}{\partial x_j}(\bar{\rho}\tilde{U}_{k,j}\tilde{Y}_k-\Phi_{k,j}^{sgs}-\Theta_{k,j}^{sgs})+\bar{\dot{\omega}}_k
\end{aligned}
\tag{2.1}
$$

The unclosed sub-grid terms are:

$$
\begin{aligned}
\tau_{ij}^{sgs}&=(\overline{\rho u_i u_j}-\bar{\rho}\tilde{u}_i\tilde{u}_j)\\
H_i^{sgs}&=(\overline{\rho E u_i}-\bar{\rho}\tilde{E}\tilde{u}_i)+(\overline{pu_i}-\bar{p}\tilde{u}_i)\\
\sigma_{ij}^{sgs}&=(\overline{u_j\tau_{ij}}-\tilde{u}_j\tilde{\tau}_{ij})\\
\Phi_{k,j}^{sgs}&=(\overline{\rho Y_k u_j}-\tilde{\rho}\tilde{Y}_k\tilde{u}_j)\\
\Theta_{k,j}^{sgs}&=(\overline{\rho Y_k U_{k,j}}-\tilde{\rho}\tilde{Y}_k\tilde{U}_{k,j})
\end{aligned}
\tag{2.2}
$$

We use block structure mesh for geometry. For sub-grid model we use Smagorinsky model [16] and a standard value of 0.7 is used for the turbulent Prandtl number. For advection term we use 5th order WENO scheme [17] which is more dissipative than the upwind scheme but quite robust for high pressure combustion simulation during our tests. For viscous term we use 6th order central difference scheme. For time iteration we use 3rd order Runge-Kutta method. For reaction source term we use finite rate reaction model with reduced mechanism and we use laminar estimation without turbulent combustion interaction. Also we use point implicit method [18] to solve stiffness of the source term. For boundary conditions we use the NSCBC [19, 20] method. RoSim has been successfully used into industrial engine design and can successfully predict combustion instabilities.

Figure 7 shows the computation domain of our simulation. Both inlet and wall are isothermal at 300K and supersonic outlet is used. The mesh size we use is 50 μm–200 μm with 10 cells at the post-lip. MPI parallel strategy [21] is used and the same grid number in each parallel zone is ensured. Figure 8 shows parallel zone of our simulation.

A 24 steps 17 species reaction mechanism [22] is used which can well predict ignition delay, flame temperature and flame speed. Figure 9 shows these three parameters change with equivalence ratio compared with detailed mechanism GRI3.0.

Figure 10 shows the normalized pressure distribution along the axis, and our simulation result is quite close to the experiment, which shows the feasibility of current method. Figure 11 shows mean temperature distribution when pc=20bar, OF=3.0. Also when gradually increasing mesh size(from 50 μm to 20 μm), there is no obvious change of simulation results.

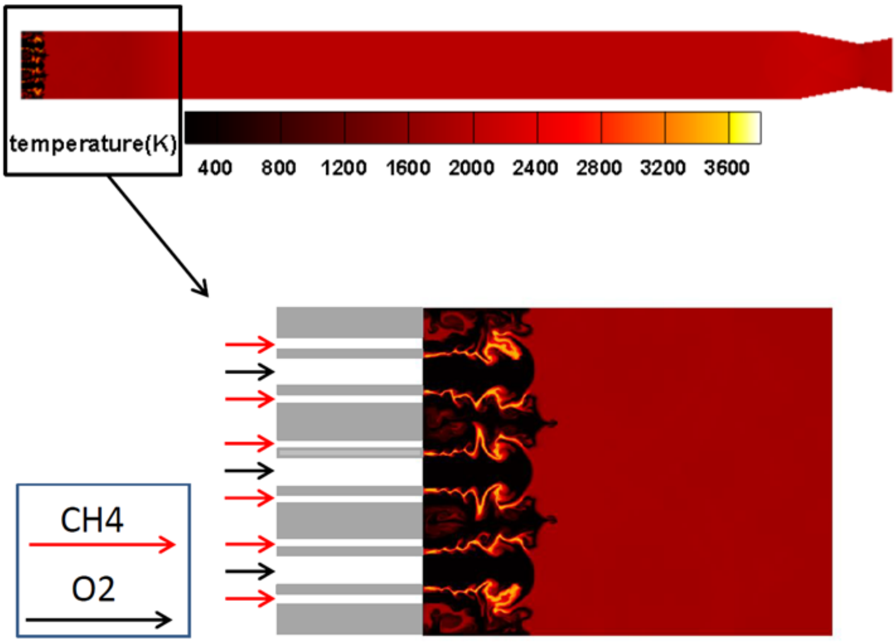

FIGURE 7. Computation domain of current simulation

FIGURE 8. Parallel zone of current simulation (same grid number in each parallel zone)

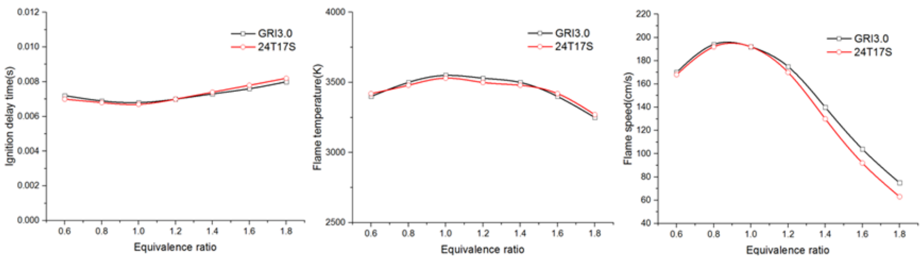

FIGURE 9. Ignition delay, flame temperature and flame speed compared with GRI3.0

3. Results

Figure 12 shows the instant temperature of the unstable case during one cycle. We can see the flame always attaches the post wall but there is an obvious fluctuation. Before the $3\pi/2$ phase the flame becomes longer and longer, with pressure wave running forwards. During the last phase, pressure wave runs quickly back to the post wall and flame becomes short very quickly. Also, there are low temperature zones in the product. This is because the cases work at fuel rich condition and there is still methane left in the product. Figure 13 shows the wall dynamic pressure at the head of the combustion chamber. We can see the pressure drops slowly but goes up quickly, which has the

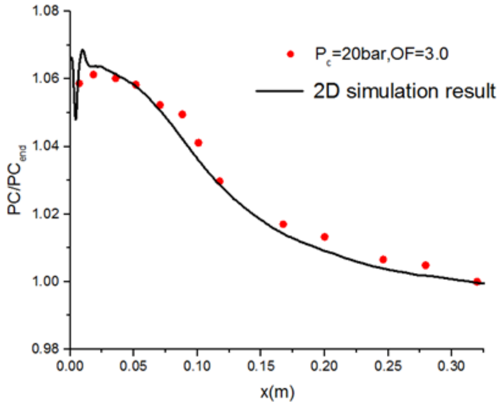

FIGURE 10. Normalized wall pressure distribution along the axis

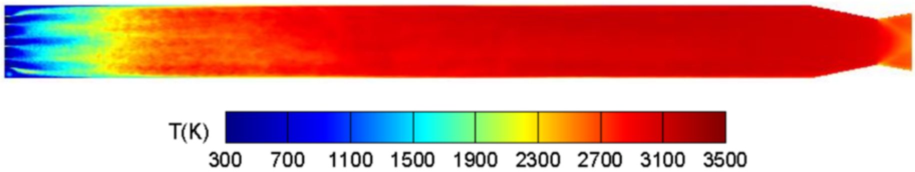

FIGURE 11. Mean temperature distribution when pc=20bar, OF=3.0

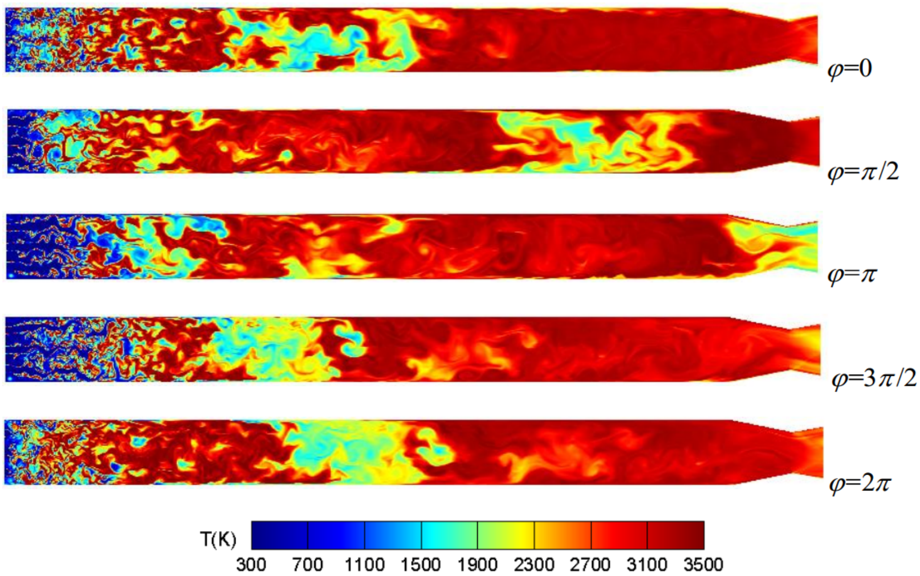

FIGURE 12. Instant temperature during one cycle (phase: $0,\pi/2,\pi,3\pi/2,2\pi$)in unstable case1

same phenomenon with temperature contours. From spectrum we can see the dominant frequency are 1470Hz with its harmonic frequencies, which is close to the experiment data(1410Hz).

Figure 14 shows instant temperature in stable case during one cycle. Compared with the unstable case, we can see the fluctuation is much less obvious and the flame length

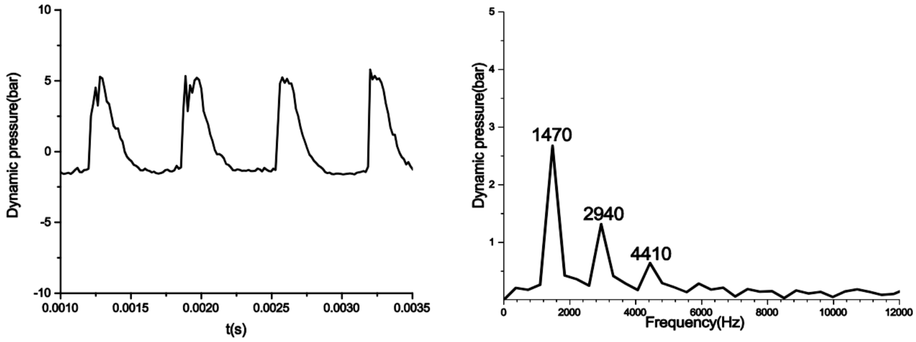

FIGURE 13. Wall dynamic pressure signal and spectrum at the head of combustion chamber in unstable case1

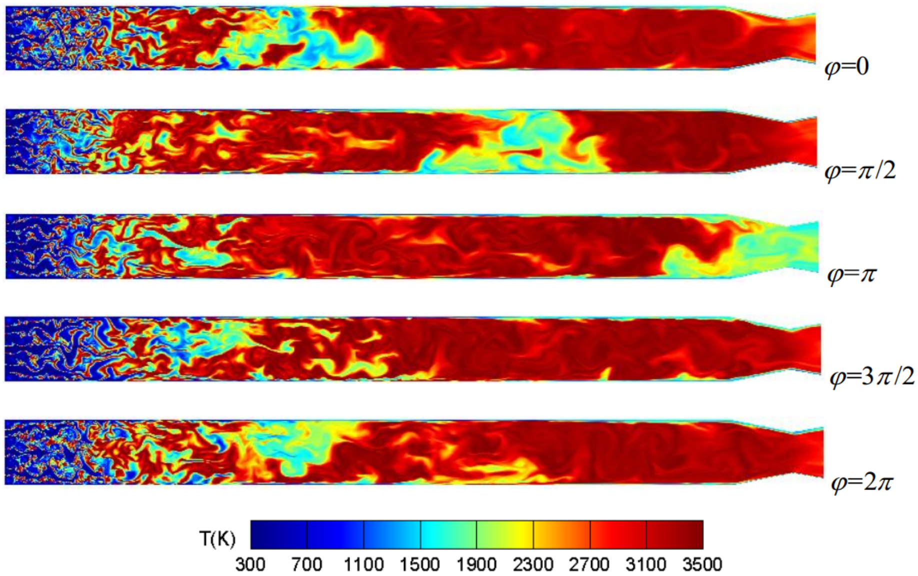

FIGURE 14. Instant temperature during one cycle (phase: $0,\pi/2,\pi,3\pi/2,2\pi$)in stable case2

changes not much. Figure 15 shows the wall dynamic pressure and we can see the amplitude is much less than the unstable case.

Since the combustion instability mainly shows the longitudinal mode, we use the average value of the transverse direction for one dimensional analysis. Figure 16 shows how the maximum of flow parameters and maximum position change with phase in unstable case. From the right figure we can see during one cycle pressure maximum runs back and forth and from the left figure this maximum reaches its peak value when it comes to the head of the combustion chamber. CH2O(which is mainly involved with the ignition process) maximum always keeps at the head of the combustion chamber and reaches the peak value when pressure wave comes, which means it has the same phase with pressure. Vorticity maximum position changes slightly with pressure wave and reaches its peak value when pressure wave comes, which means pressure wave will increase the vorticity and then increase fuel oxygen mixing, thus promoting combustion and heat release. This is because the pressure will increase the baroclinic term of the vortic-

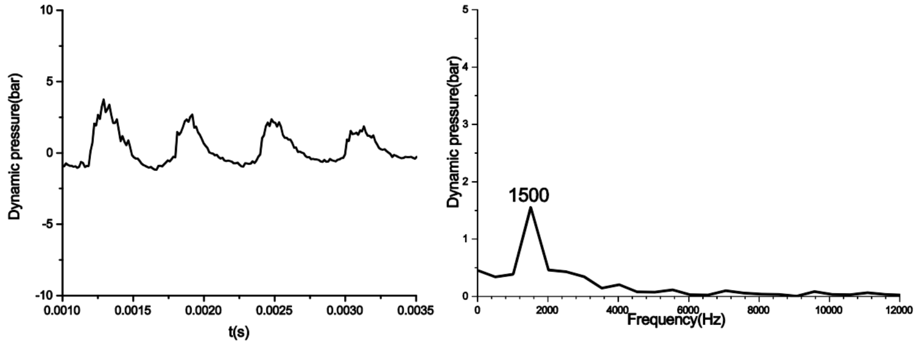

FIGURE 15. Wall pressure signal and spectrum at the head of combustion chamber in stable case2

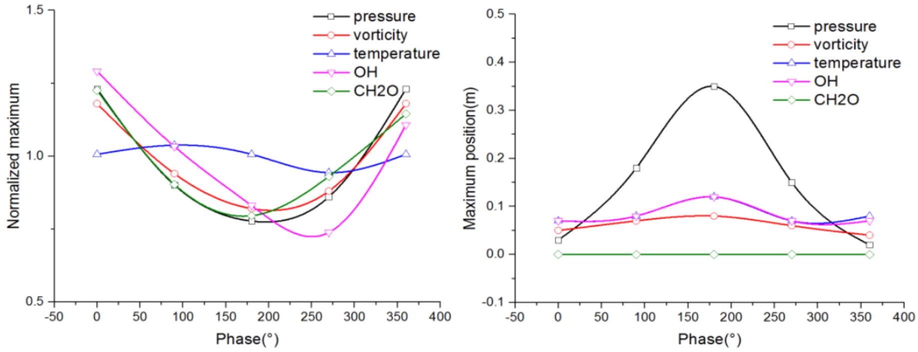

FIGURE 16. Normalized maximum of flow parameters and maximum position in unstable case1

ity equation and then increase the vorticity. OH(which is mainly involved with the heat release) maximum position changes with pressure and reaches a high value when pressure wave comes, and the peak value has a phase lag with pressure or CH2O(less than $90°$), which means it is still mostly coupling with pressure.

Figure 17 shows how the maximum of flow parameters and maximum position change with phase in stable case. From the right figure we can see pressure maximum runs back and forth in the whole chamber but from the left figure this maximum reaches peak value at the end of the combustion chamber rather than at the head. CH2O maximum keeps near the post wall but does not reach peak value anymore when pressure wave comes. Also, vorticity maximum position does not change much and has totally different phase with pressure. OH also has different phase with pressure. In this stable case, there is no obvious coupling between pressure and combustion process, thus the pressure oscillation becomes much weaker.

4. Conclusions

Large eddy simulation of a multi-injector GOX/GCH4 combustor has been used to predict combustion instabilities and pressure distribution along the axis has been compared with experiment data. Both stable and unstable cases are predicted by numerical simulation, and the thermoacoustic coupling has been invested.

For the unstable case, the dominant frequency is close to the experiment, and the

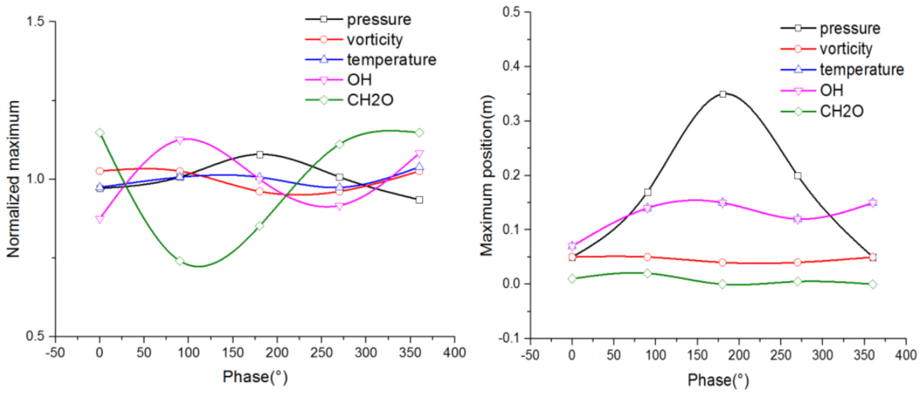

FIGURE 17. Normalized maximum of flow parameters and maximum position in stable case2

flame length increases slowly but decrease quickly. Since the cases work at fuel rich zone, there is still unburnt methane left, causing low temperature field in the product. For the stable case, the pressure amplitude is much smaller and the flame length does not change much during one cycle.

For the unstable case, when pressure wave comes to the head of the chamber, CH2O reaches its peak value, and vorticity also reaches its peak value because pressure gradient increases the baroclinic term of the vorticity equation. This vorticity increment will increase fuel oxygen mixing, thus promoting combustion and heat release. OH reaches a high value when pressure wave comes, and there is a phase lag which is less than $90°$. Pressure and heat release are mostly coupled, leading to combustion instabilities. For stable case, there is no obvious coupling between pressure and combustion process, thus the pressure amplitude is much weaker.

Futher explaining the coupling mechanism requires to understand the relationship among several time scales, which is the mixing time, the cold inflow heating time, ignition delay time, and acoustic propagation time. A theoretical model should be build based on time-lag theory, which is worth being studied in the future.

Acknowledgments

Financial support has been provided by the German Research Foundation (Deutsche Forschungsgemeinschaft – DFG) in the framework of the Sonderforschungsbereich Transregio 40. Computational resources have been provided by central computing facility (LRZ) at TUM and high performance computing center at Chinese Academy of Science.

References

[1] SILVESTRI, S., CELANO, M.P., SCHLIEBEN, G. AND HAIDN, O.J. (2016). Characterization of a multi-injector gox-gch4 combustion chamber. In: *Joint Propulsion Conference, JPC2016*.

[2] VALLER, H. (1979). Design, fabrication and delivery of a high pressure lox-methane injector.

[3] LOCKE, J.M., PAL, S. AND WOODWARD, R.D. (2007). Chamber wall heat flux measurements for a lox/ch4 uni-element rocket. *AIAA Paper*, **5547**, 2007.

[4] BONHOMME, C., THERON, M., LOUAAS, E., BEAURAIN, A. AND SELEZNEV, E. (2006). French–russian activities in the lox/lch4 area. In: *57th IAF Congress, Valencia*.

[5] LUX, J., SUSLOV, D., BECHLE, M., OSCHWALD, M. AND HAIDN, O. (2006). Investigation of sub-and supercritical lox/methane injection using optical diagnostics. *AIAA Paper*, **5077**, 2006.

[6] SEEDHOUSE, E. (2013). *SpaceX: making commercial spaceflight a reality*. Springer Science & Business Media.

[7] CELANO, M., SILVESTRI, S., BAUER, C., PERAKIS, N., SCHLIEBEN, G. AND HAIDN, O. (2016). Comparison of a single and multi-injector gox-gch4 combustion chamber. *AIAA*.

[8] SILVESTRI, S., SCHLIEBEN, G., KIRCHBERGER, C., HAIDN, O., HÖGLAUER, C. AND KNAB, O. Experimental and numerical investigations on film cooling and heat transfer in a rocket combustion chamber.

[9] SELLE, L., BLOUQUIN, R., THÉRON, M., DOREY, L.H., SCHMID, M. AND ANDERSON, W. (2014). Prediction and analysis of combustion instabilities in a model rocket engine. *Journal of Propulsion and Power*.

[10] ROTH, C., HAIDN, O., CHEMNITZ, A., SATTELMAYER, T., DAIMON, Y., FRANK, G., MÜLLER, H., ZIPS, J., PFITZNER, M., KELLER, R. ET AL. (2016). Numerical investigation of flow and combustion in a single-element gch4/gox rocket combustor. In: *52nd AIAA/SAE/ASEE Joint Propulsion Conference*. 4995.

[11] MÜLLER, H., ZIPS, J., PFITZNER, M., MAESTRO, D., CUENOT, B., SELLE, L., RANJAN, R., TUDISCO, P. AND MENON, S. (2016). Numerical investigation of flow and combustion in a single-element gch4/gox rocket combustor: A comparative les study. In: *52nd AIAA/SAE/ASEE Joint Propulsion Conference*. 4997.

[12] ROTH, C., HAIDN, O., RIEDMANN, H., IVANCIC, B., MAESTRO, D., CUENOT, B., SELLE, L., DAIMON, Y., CHEMNITZ, A., KELLER, R. ET AL. (2015). Comparison of different modeling approaches for cfd simulations of a single-element gch4/gox rocket combustor. *Sonderforschungsbereich/Transregio 40, Summer Program Report 2015*.

[13] TERASHI, H., DAIMON, Y., ÅŔŽÅŞŰÆŤŃÅŔŠ AND ÅĎĞÉŰĂÅĎŁ (2015). Combustion modeling study for a gch4/gox single element combustion chamber: unsteady simulations. *title Proceedings of the 2015 Summer Program*, 151.

[14] ZIPS, J., MÜLLER, H., FRANK, G. AND PFITZNER, M. Numerical simulation of a single-element gox/gch4 rocket combustion chamber using a non-adiabatic flamelet/progress variable approach.

[15] MAESTRO, D., SELLE, L. AND CUENOT, B. Thermally chained les of a gch4/gox single element combustion chamber.

[16] HUANG, Y., SUNG, H.G., HSIEH, S.Y. AND YANG, V. (2003). Large-eddy simulation of combustion dynamics of lean-premixed swirl-stabilized combustor. *Journal of Propulsion and Power*, **19**(5), 782–794.

[17] JIANG, G.S. AND SHU, C.W. (1996). Efficient implementation of weighted eno schemes. *Journal of computational physics*, **126**(1), 202–228.

[18] BUSSING, T. AND MURMAN, E. (1988). Finite-volume method for the calculation of compressible chemically reacting flows. *AIAA journal*, **26**(9), 1070–1078.

[19] POINSOT, T.J. AND LELEF, S. (1992). Boundary conditions for direct simulations of compressible viscous flows. *Journal of computational physics*, **101**(1), 104–129.

[20] POINSOT, T. AND VEYNANTE, D. (2005). *Theoretical and numerical combustion*.

RT Edwards, Inc.

[21] GROPP, W., LUSK, E. AND SKJELLUM, A. (1999). *Using MPI: portable parallel programming with the message-passing interface*, vol. 1. MIT press.

[22] LI, S. AND WILLIAMS, F. (2000). Reaction mechanisms for methane ignition. In: *ASME Turbo Expo 2000: Power for Land, Sea, and Air*. American Society of Mechanical Engineers, V002T02A061–V002T02A061.